JOC The Journal of Organic Chemistry

Article

pubs.acs.org/joc

Application of Radical Cation Spin Density Maps toward the Prediction of Photochemical Reactivity between *N*-Methyl-1,2,4-triazoline-3,5-dione and Substituted Benzenes

Gary W. Breton* and Kevin R. Hoke

Department of Chemistry, Berry College, 2277 Martha Berry Highway, Mount Berry, Georgia 30149, United States

Supporting Information

ABSTRACT: Visible light irradiation of *N*-methyl-1,2,4-triazoline-3,5-dione in the presence of substituted benzenes is capable of inducing substitution reactions where no reaction takes place thermally. In addition to the formation of 1-arylurazole products resulting from ring substitution, side-chain substitution occurs in some cases where benzylic hydrogens are accessible to form benzylic urazole products. Formation of both types of products is most consistent with the involvement of a common intermediate, a radical ion pair, generated from photoexcitation of an initially formed charge-transfer complex. The charge-transfer complexes have been observed spectroscopically. Additionally, application of a modified Rehm−Weller model suggests that the electron-transfer processes are feasible for all of the substrates examined. In most cases, the spin density maps of the aromatic radical cation intermediates calculated at the DFT UB3LYP/6-31G* level are excellent predictors of the observed product distributions.

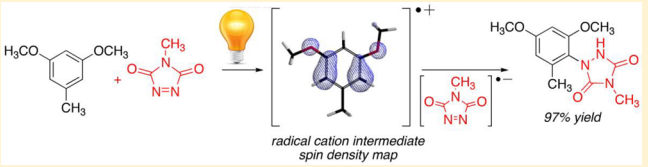

INTRODUCTION

1-Arylurazoles (**1**, Scheme 1) are heterocyclic compounds with potential applications as vasodilators, anticonvulsants, and analgesics.[1] Additionally, oxidation of urazoles is known to give rise to an interesting class of N-centered persistent radicals.[2]

Scheme 1. Formation of 1-Arylurazoles (1) via Reaction of *N*-Methyl-1,2,4-triazoline-3,5-dione (2) with Substituted Benzenes

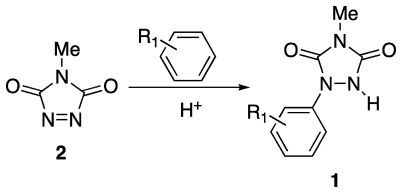

We recently described a method for the synthesis of 1-arylurazoles via addition of *N*-methyl-1,2,4-triazoline-3,5-dione (**2**) to substituted benzenes using trifluoroacetic acid as catalyst (Scheme 1).[3] **2** is a red crystalline compound that forms characteristic pinkish red solutions when dissolved in commonly used organic solvents. We considered the possibility of synthesizing 1-arylurazoles by promoting the reactivity of **2** with substituted benzenes by photochemical means (using visible light) rather than via the addition of catalysts. Visible light irradiation of solutions of RTADs alone in unreactive solvents (e.g., CCl_4, CH_2Cl_2, EtOAc) is reported to result in rapid decomposition and/or polymerization of the triazoline-dione.[4] Irradiation of RTADs in the presence of ethers, however, leads to formation of substituted urazoles **3**, presumably via initial hydrogen atom abstraction at the position α to the oxygen in the ether substrate (Scheme 2).[4c,5] In contrast, it was reported that irradiation of *N*-phenyl-1,2,4-triazoline-3,5-dione (PhTAD, Scheme 2) in anisole as the solvent led to formation of 1-arylurazole **4**, albeit in low yield (16%).[4c] Sheridan reported that visible light irradiation of **2** in the presence of naphthalene, phenanthrene, and (at low temperatures) benzene led to formation of Diels−Alder adducts **5**−**7**, respectively (Figure 1).[6] Both the singlet and triplet excited states of **2** were implicated in the reactions.[6a,b] Our laboratory later reported that **2** reacts both thermally and

Scheme 2. Photochemical Reactions of RTADs with Ethers

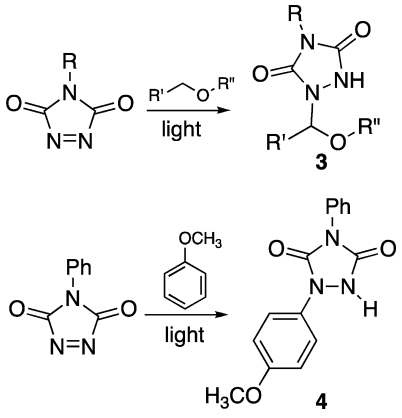

Received: January 22, 2013
Published: April 17, 2013

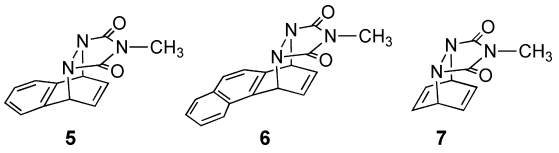

5 6 7

Figure 1. Diels–Alder photoadducts of **2** with aromatic substrates.

photochemically (visible light irradiation) with substituted naphthalenes via a Diels–Alder cycloaddition.[7] Finally, RTADs have been shown to engage in Diels–Alder type photoreactions with the aromatic rings of naphtho[1,2,3,4-*def*]chrysene and C_{60}.[8,9] While the photochemical reactions of RTADs have been further explored,[10] we were unable to locate any additional studies of photochemical reactions of RTADs with substituted benzenes. Herein we report upon our investigations of the photochemical reaction of **2** with a series of substituted benzenes.

RESULTS AND DISCUSSION

1. Photochemical Reaction of MeTAD (2) with Substituted Benzenes. RTADs are known to react thermally, in the absence of catalysts, with some electron-rich aromatic compounds to form 1-arylurazoles.[8,11] For example, Hall reported the thermal reaction of PhTAD with 1,3,5-trimethoxybenzene to afford the corresponding 1-arylurazole **8**.[11c] Similarly, when we added **2** to 1.5 equiv of 1,3,5-trimethoxybenzene in CH_2Cl_2 at room temperature in the absence of light, a deep blood red coloration of the reaction mixture was observed, presumably due to formation of a charge-transfer complex with the aromatic compound. The formation of charge-transfer complexes between RTADs and aromatic compounds is well-known (see below).[6b,7,11] The color was slowly discharged over a 9 h period with concomitant formation of 1-arylurazole **9** (Table 1) in 90% yield. However, when an identical reaction mixture was subjected to visible-light irradiation with three 300 W incandescent bulbs (in Pyrex glassware with temperature maintained at 20 °C via external cooling), the deep red color of the charge transfer complex was discharged within just 0.5 h, and **9** was isolated in a comparable 87% yield (Table 1).

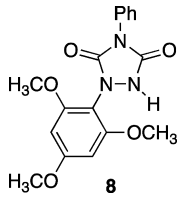

8

Similarly, while the thermal reaction of **2** with 1,3-dimethoxybenzene over 4 days afforded a 46% yield of **10**, irradiation of an identical reaction mixture provided a 70% yield of **10** in just 3 h. Surprisingly, irradiation of **2** in the presence of 1,4-dimethoxybenzene for 48 h failed to form any urazole products. In addition to recovered starting materials, photodecomposition products of **2** were observed. Interestingly, Hall also remarked upon the reluctance of PhTAD to engage in a thermal reaction with 1,4-dimethoxybenzene, in contrast to its ready reaction with both 1,3,5-trimethoxybenzene and 1,3-dimethoxybenzene.[11c] There was no observed thermal reaction between 3-methylanisole and **2** over several days, but irradiation for 18 h led to formation of 1-arylurazole **11a** as the major product (62% yield) along with lesser amounts (17% yield) of two other ring-substituted products in an approximate 1:1 ratio. In contrast, urazole **11a** was the sole regioisomer formed in the acid-catalyzed reaction of **2** with 3-

Table 1. Photochemical Reaction of 2 with Substituted Benzenes

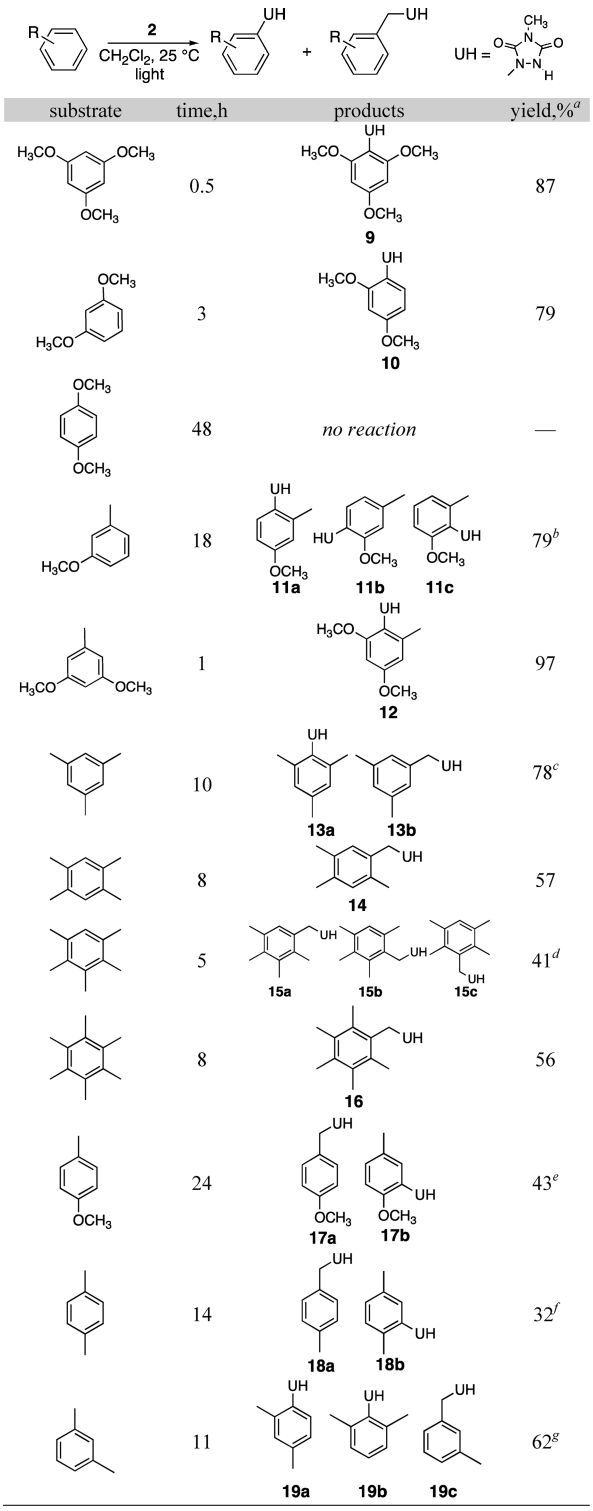

substrate	time,h	products	yield,%[a]
1,3,5-trimethoxybenzene	0.5	**9**	87
1,3-dimethoxybenzene	3	**10**	79
1,4-dimethoxybenzene	48	*no reaction*	—
3-methylanisole	18	**11a** **11b** **11c**	79[b]
1,3,5-trimethoxybenzene	1	**12**	97
toluene	10	**13a** **13b**	78[c]
ethylbenzene	8	**14**	57
cumene	5	**15a** **15b** **15c**	41[d]
tert-butylbenzene	8	**16**	56
anisole	24	**17a** **17b**	43[e]
n-propylbenzene	14	**18a** **18b**	32[f]
n-butylbenzene	11	**19a** **19b** **19c**	62[g]

[a]Isolated yields; ratios determined either by chromatographic separation of individual isomers or by ^{1}H NMR integration (see the Experimental Section). [b]Ratio **11a**:**11b**:**11c** = 78:11:11. [c]Ratio **13a**:**13b** = 70:30. [d]Two major isomers (**15a**/**15b**) and one minor isomer (**15c**) were observed. [e]Ratio **17a**:**17b** = 83:17. [f]Ratio **18a**:**18b** = 94:6. [g]Ratio **19a**:**19b**:**19c** = 52:26:22.

dx.doi.org/10.1021/jo4001417 | J. Org. Chem. 2013, 78, 4697–4707

Scheme 3. Kochi's Mechanism for Formation of Ring- and Side-Chain-Substituted Products via a Common Radical Cation Intermediate

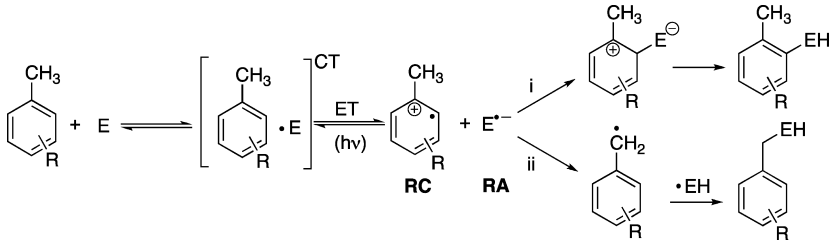

methylanisole.[3] The regiochemistry of **11a** was verified by an HMBC NMR experiment. The two minor products exhibited signals in the ^{1}H NMR spectrum that are consistent with the ring-substituted structures **11b**,**c**. The presence of the other possible regioisomer, **11d**, is *not* consistent with the observed signals. The chemical shifts of the aromatic ring protons in the ^{1}H NMR spectrum for **11d** are predicted to be three broadened singlets (due to ineffectual meta coupling) at ~7.1, 6.9, and 6.6 ppm.[12] Instead, all of the observed aryl proton signals appear as distinct multiplets, and these observed multiplets correlate better with the predicted shifts and multiplicities for structures **11b**,**c**. Finally, irradiation of a solution of **2** and 3,5-dimethoxytoluene regioselectively afforded **12** in 97% yield (Table 1). Thus, as originally hypothesized, simple visible light irradiation of reaction mixtures of **2** and these substituted benzenes either increased the rate of the substitution reaction relative to the thermal reaction or allowed for reactivity that was otherwise thermally absent.

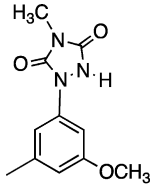

11d

We earlier reported that the acid-catalyzed reaction of **2** with mesitylene leads to formation of 1-arylurazole **13a** in 99% yield.[3] Interestingly, however, the photochemical reaction of **2** with mesitylene resulted in the formation of *two* products (Table 1). The major product (55% yield) was the same product (**13a**) formed in the acid-catalyzed reactions. However, also isolated was the side-chain-substituted urazole **13b** (23% yield). The structure of the benzylic-substituted compound **13b** was confirmed by an independent synthesis (see the Experimental Section).

The photochemical reaction of **2** with durene afforded only benzylic urazole **14**. Similarly, irradiation of **2** in the presence of pentamethylbenzene yielded a mixture of the three possible benzylic-substituted compounds **15a**–**c** (total of 41% yield) without any formation of ring-substituted product, despite the predilection of pentamethylbenzene toward electrophilic aromatic substitution (EAS). We were unsuccessful at separating these isomeric urazoles, but from the ^{1}H NMR spectrum of the mixture, there were obviously three regioisomers present in an approximate ratio of 4:3:1. The spectrum displayed three distinct aryl singlets and three benzylic CH_2 signals. While only two *N*-Me signals were observed, one had an obvious shoulder, suggesting partial overlap of two signals. Furthermore, given the symmetry of compound **15c** versus compounds **15a**,**b**, there are a total of 10 signals expected for the methyl groups on the aromatic rings, and, indeed, 10 distinguishable signals were observed. The integrations for the combination of these signals were internally consistent with a mixture of three products in a 4:3:1 ratio. By making use of the relative integrations, it was possible to assign complete ^{1}H NMR data for each of the three compounds (see the Experimental Section). According to these assignments, the minor compound most probably has structure **15c**.

Hexamethylbenzene, for which ring substitution is impossible, yielded the benzylic urazole **16** upon irradiation. Photoreaction of 4-methylanisole with **2** resulted in the formation of primarily benzylic urazole **17a** (36% yield) along with a smaller amount of the 1-arylurazole **17b** (7% yield). This behavior contrasts with the reactivity observed for the other methoxy-substituted benzenes, for which only ring substitution was observed. The regiochemistry of **17b** was consistent with HMBC NMR experiments. Similarly, *p*-xylene afforded a 30% yield of benzylic urazole **18a** and only a 2% yield of the 1-arylurazole **18b**. Finally, reaction with *m*-xylene yielded a nearly inseparable mixture of three products **19a**–**c** in an approximate 2:1:1 ratio. Urazole **19a** had been isolated previously as the sole reaction product from the thermal acid-catalyzed reaction of **2** with *m*-xylene and was readily identified.[3] Chromatographic fractions could be enriched in mixtures of **19a** and **19b** for analysis by NMR spectroscopy. The structure for **19b** was assigned by subtracting the signals due to **19a** from the ^{1}H and ^{13}C NMR spectra of the mixture. The magnitude of the coupling constants observed in the aromatic region of the ^{1}H NMR spectrum (7.8 Hz) are consistent with ortho-coupled protons as would be present in structure **19b**, and not with meta-coupled protons present in the remaining possible regiosomer **19d**.

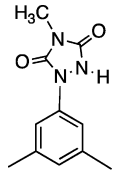

19d

In all of the reactions that resulted in formation of benzylic urazoles, varying amounts of *N*-methylurazole (i.e., reduced **2**) were also observed. We made no attempt to quantify the amount of *N*-methylurazole formed, due to its low solubility in organic solvents and its reluctance to elute cleanly on chromatographic columns.

2. Competition between Ring and Side-Chain Substitution Observed in the Reactions of Substituted Benzenes with Other Electrophiles. In our previous work on acid-catalyzed reactions of **2** with substituted benzenes, we assumed the 1-arylurazole products to be the result of a typical

dx.doi.org/10.1021/jo4001417 | J. Org. Chem. 2013, 78, 4697–4707

EAS process. Similarly, the 1-arylurazoles formed in the photochemical reactions might be envisioned to arise from a straightforward EAS process in which photoactivated **2** serves as the electrophile. However, the observed benzylic urazole products must necessarily derive from a different process.

In a series of seminal papers, Kochi investigated the formation of side-chain-substituted products in competition with ring-substituted products during the thermal reactions of methylated benzenes with electrophiles such as Cl_2, NO_2^+, and $Tl(O_2CCF_3)_3$, as well as in photochemical reactions with *N*-nitropyridinium salts and tetranitromethane.[13] Formation of both the ring-substituted and side-chain-substituted products were attributed to the intermediacy of radical cations (RCs) formed from the aromatic substrates via electron transfer from within an initially formed charge-transfer (CT) complex (Scheme 3). Kochi postulated that cage collapse of the radical anion (RA)—formed from one-electron reduction of the electrophile—with the RC yields a Wheland complex (route i in Scheme 3), which then results in formation of the observed ring-substituted products. Alternatively, deprotonation of a benzylic hydrogen from the RC by the RA (or externally added base) affords a pair of reactive radicals (route ii), from which the observed side-chain-substituted products are derived. Furthermore, Kochi demonstrated that direct irradiation of the CT complex stimulated electron transfer in several cases where the CT complex was unable to undergo spontaneous electron transfer to form RC/RA intermediates (i.e., in the reactions with tetranitromethane and *N*-nitropyridinium).[13b,c] In order to ascertain whether a similar mechanism might be involved in the photochemical reactions between **2** and the substituted benzenes, we sought to better characterize the charge-transfer complexes formed between the two.

3. Evidence for the Formation of Charge-Transfer Complexes between 2 and Substituted Benzenes. As noted earlier, charge-transfer complexes have been previously observed in the reactions of RTADs with suitably electron rich aromatic compounds.[6b,7,11] In most of the reactions that we studied, there was an obvious visual darkening of the reaction mixture to form deep red solutions upon combining **2** with the aromatic substrate. We were able to directly observe charge-transfer complexes formed between **2** and several of the aromatic substrates studied by mixing solutions of **2** (10 mM) and an excess of substrate (~1 M) in CH_2Cl_2 and examination by difference UV–vis spectroscopy. The absorption band derived for the CT complex between **2** and mesitylene is displayed in Figure 2 as a representative example. Data for CT complexes formed from other methylated benzenes are presented in Table 2. A plot of the absorption band energies (E_{CT}) with the ionization potentials (IP) of the aromatic substrates afforded a good correlation (R^2 = 0.93), as shown in Figure 3.[14] Energies of the absorption bands were observed to decrease with decreasing ionization potential of the substrates (Figure 3), which is consistent with what would be expected for charge transfer from the electron-rich aromatic substrate to the electrophilic triazolinedione **2**. Furthermore, the absorption energies of the CT bands from **2** correlate fairly well (R^2 = 0.83) with the energies of the absorption bands formed between the same arenes and the electrophile I_2 (Figure 4), which have been previously established to derive from a charge-transfer interaction.[15] This further corroborates the charge-transfer nature of the observed UV–vis absorptions of **2**.

4. Possible Mechanism for the Photochemical Reaction of 2 with Substituted Benzenes. It is conceivable

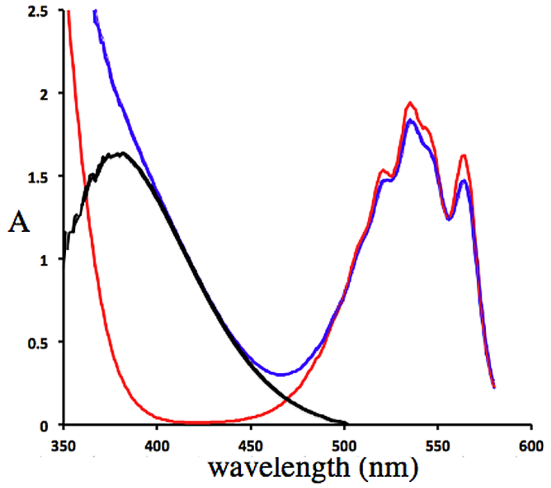

Figure 2. UV–vis spectral absorption of the charge-transfer complex (in black) between MeTAD (**2**) and mesitylene, as generated by subtracting the absorption of **2** alone (in red) from that of a mixture of **2** and mesitylene (in blue). Absorption by mesitylene alone in this region of the spectrum is negligible.

Table 2. Spectral Data for Charge Transfer Complexes between 2 and a Series of Methylated Benzenes in CH_2Cl_2

substrate	IP,[a] eV	λ_{CT},[b] nm	E_{CT}, eV
hexamethylbenzene	7.85	437	2.84
pentamethylbenzene	7.92	414	2.99
durene	8.07	396	3.13
mesitylene	8.41	379	3.27
p-xylene	8.52	375	3.31
m-xylene	8.56	366	3.39

[a]Ionization potential.[14] [b]λ_{max} of the CT absorption band.

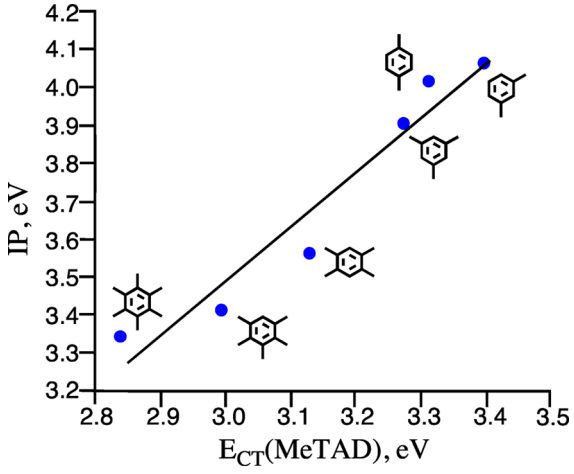

Figure 3. Correlation of the observed energies of the charge-transfer absorption bands formed between **2** and various methylated benzenes (E_{CT}(MeTAD)) with the ionization potentials of the substrates.

that irradiation of the CT complexes formed between **2** and the substituted benzenes leads to electron transfer to form the RC of the electron-rich aromatic substrate and the radical anion (RA) of **2** (Scheme 4).[16] The resulting radical ion pair may then follow the two pathways analogous to those previously mapped by Kochi (Scheme 4):[13] i.e., collapse of the radical ion pair to form a Wheland intermediate which proceeds to form the observed 1-arylurazole products (route i) or deprotonation

dx.doi.org/10.1021/jo4001417 | J. Org. Chem. 2013, 78, 4697–4707

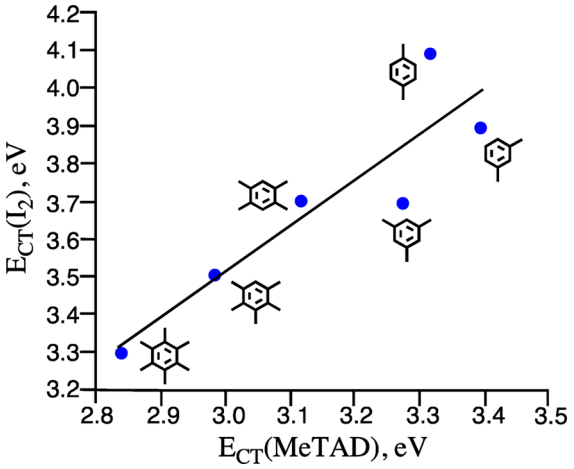

Figure 4. Correlation of the observed energies of the charge-transfer absorption bands formed for various methylated benzenes with **2** (E_{CT}(MeTAD)) and those with iodine ($E_{CT}(I_2)$).

of a benzylic proton from the aromatic RC by the RA of **2** followed by collapse of the newly generated radicals to form the observed benzyl urazole products (route ii). The feasibility of electron transfer from the aromatic substrate to photoexcited **2** may be estimated by application of the Rehm−Weller model, as recently re-examined by Farid.[17] According to this model, the effective free energy change for the electron transfer process ($\Delta G'$) may be estimated by employing the equation

$$\Delta G' = [E(\mathrm{Ar}^+/\mathrm{Ar}) - E(\mathbf{2}/\mathbf{2}^{\bullet-})] - E_{\mathrm{excit}} + 0.08\ \mathrm{eV} \quad (1)$$

where $E(\mathrm{Ar}^+/\mathrm{Ar})$ is the potential required to oxidize the aromatic substrate, $E(\mathbf{2}/\mathbf{2}^{\bullet-})$ is the reduction potential of **2**, E_{excit} is the energy of excitation for **2** (2.29 eV for **2** in the singlet excited state),[18] and the constant in the equation reflects the estimated combined effects of Coulombic stabilization and desolvation energies of the newly generated RC/RA pair in dichloromethane (i.e., the same solvent in which E_{excit} for **2** was obtained).[19] Application of this equation to a reaction of interest requires knowing the difference in potential between the electron donor and acceptor. However, we were not able to find consistent values for the reduction potential of **2** in the literature. While Bausch reported a value of 0.31 V (corrected to SHE) in DMSO,[20] more recently Volanschi reported a value of −0.042 V in the same solvent.[21] No explanation for this discrepancy was provided, and without a ferrocene reference or other internal standard for the latter work, direct comparisons are difficult. In addition, most of the potentials reported for the aromatic substrates were obtained using acetonitrile as solvent rather than DMSO.[22] Although Volanschi did report a value for the reduction of **2** in acetonitrile (−0.153 V corrected to SHE),[21] the large difference between the two reported potential values in DMSO gives concern that the reduction potential reported for **2** in acetonitrile might also not correspond to measurements made by others. For example, significant junction potentials can exist between the typical aqueous reference electrodes and anhydrous electrolytes used in electrochemical cells.[23] These liquid junction potentials can vary, depending on the construction of the cells and the reference electrodes. Therefore, we carried out cyclic voltammetry for both **2** and the aromatic donors ourselves to eliminate any environmental variations that could lead to errors in the measured difference in potential between the electron donor and acceptor.

5. Electrochemical Studies of 2 and the Substituted Benzenes. We observed the same electrochemical behavior for **2** as reported by Volanschi, as shown in Figure 5A.[21] The key feature is a reversible signal that is observed at a potential 0.467 V lower than that of ferrocene. This corresponds to 0.158 V vs SHE, corrected on the basis of a ferrocene potential of 0.624 V vs SHE.[24] This value is much higher than that reported by Volanschi, but they did not utilize an internal standard, such as ferrocene, for verification. However, the potential of **2** in DMSO reported by Bausch is 0.44 V less than was observed for ferrocene, which is similar to the difference that we observe. By using a ferrocene internal standard for all our measurements, we were able to compare directly the potentials for **2** and the series of prospective aromatic electron donors.

Following each measurement, ferrocene was added to the cell and a reference voltammogram was obtained. The average ferrocene potential was measured at 0.470 V vs our silver chloride reference electrode. This potential only varied by ±3 mV for the data collected. There exists a great variation in the reported potentials for ferrocene, even under similar conditions.[22c,24] We used a potential of 0.624 V vs SHE for ferrocene to convert potentials to the standard hydrogen electrode as needed.[24] Potentials derived in this manner for the aromatic substrates were about 50 mV lower than those reported elsewhere under similar conditions.[25] However, the primary parameter we seek is the *difference* in potential between these aromatic electron donors and **2**. For this purpose no corrections other than referencing to ferrocene are necessary, as we used the same experimental conditions for all of our measurements.

With the exception of 1,4-dimethoxybenzene, all of the oxidations were nonreversible for sweep rates up to 0.1 V/s.

Scheme 4. Proposed Mechanism for Formation of Ring- and Side-Chain-Substituted Products from Irradiation of Charge-Transfer Complexes between 2 and Substituted Benzenes

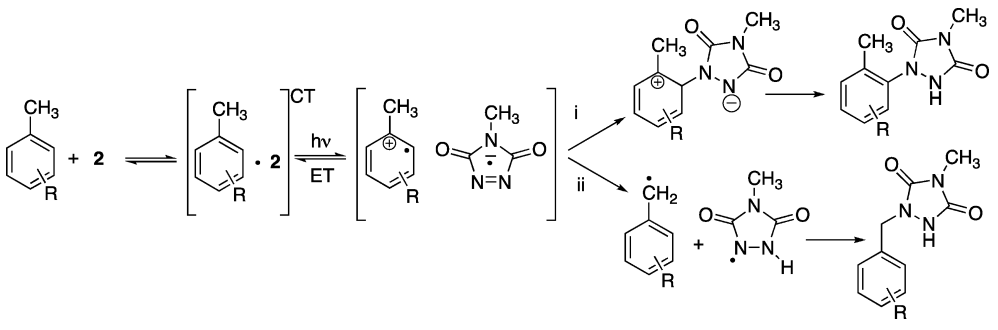

dx.doi.org/10.1021/jo4001417 | J. Org. Chem. 2013, 78, 4697−4707

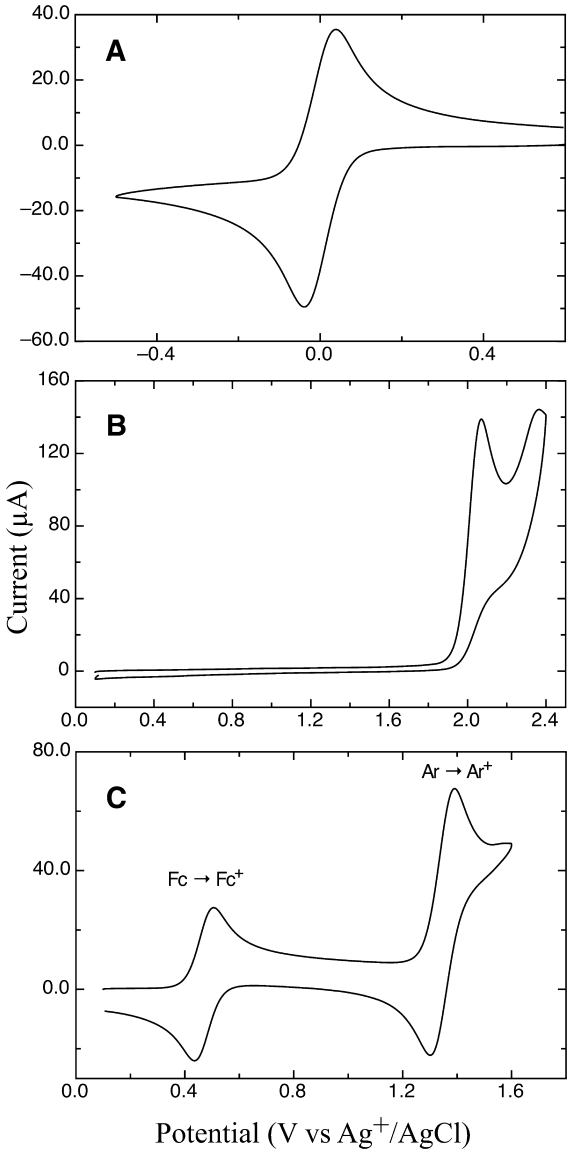

Figure 5. Cyclic voltammograms determined at 0.1 V/s in 0.1 M $TBAPF_6$ in acetonitrile: (A) **2** (1.7 mM); (B) mesitylene (1.5 mM); (C) 1,4-dimethoxybenzene (1.6 mM) with ferrocene (0.4 mM). Potentials were measured against a reference of Ag/AgCl in KCl(aq), for which ferrocene gave an observed potential of 0.470 V.

The cyclic voltammogram of mesitylene is provided in Figure 5B as a representative example. Oxidation of the aromatic substrates took place uneventfully, but generally the corresponding reduction of the RC was not observed. Apparently the RCs generated via the oxidative process are consumed rapidly, either by a polymerization process or by trapping with acetonitrile,[26,27] thereby preventing observation of the reductive couple. Unlike the other substrates, however, oxidation of 1,4-dimethoxybenzene at 0.1 V/s is quasi-reversible ($E_{1/2}$ = 1.49 V). The current observed for the oxidation was somewhat greater than the current for reduction of the RC, indicating that while annihilation of the RC does occur, it does so at a significantly slower rate than for the other RCs (Figure 5C).[27−29] It is apparent from the voltammetry that the RC of 1,4-dimethoxybenzene is much less prone to reaction with external nucleophiles than are the RCs of the other substrates investigated. Table 3 contains the experimentally determined peak potentials for all of the aromatic substrates studied in the photochemical reactions with **2**.

Table 3. Potentials of Investigated Aromatic Substrates and Estimation of the Feasibility of Electron Transfer from within the Charge-Transfer Complex by Application of the Modified Rehm−Weller Model

substrate	$E_{pa}{}^{a}$ (V)	$\Delta G'^{b}$ (eV)
hexamethylbenzene	1.79	−0.57
pentamethylbenzene	1.89	−0.48
durene	1.96	−0.41
mesitylene	2.22	−0.15
p-xylene	2.21	−0.16
m-xylene	2.32	−0.05
1,3,5-trimethoxybenzene	1.61	−0.76
1,3-dimethoxybenzene	1.71	−0.66
1,4-dimethoxybenzene	1.54	−0.83
3,5-dimethoxytoluene	1.66	−0.71
p-methylanisole	1.83	−0.53
m-methylanisole	1.89	−0.48

[a]Peak potentials (corrected to SHE) as determined by cyclic voltammetry for 1−3 mM substrate in acetonitrile with 0.1 M $TBAPF_6$ using an aqueous Ag/AgCl reference electrode in KCl. The potential of ferrocene under these conditions was observed at 0.470 V and then corrected to 0.624 V vs SHE. [b]Calculated using eq 1 by applying the $E_{1/2}$ reduction potential of **2** (0.16 V vs SHE) as determined under the same conditions.

A plot of the charge transfer absorption band energies (E_{CT}) of the series of methylated benzenes (Table 2) with the anodic (oxidative) peak potentials (E_{pa}) for the aromatic substrates affords a strong correlation (R^2 = 0.96), as shown in Figure 6.

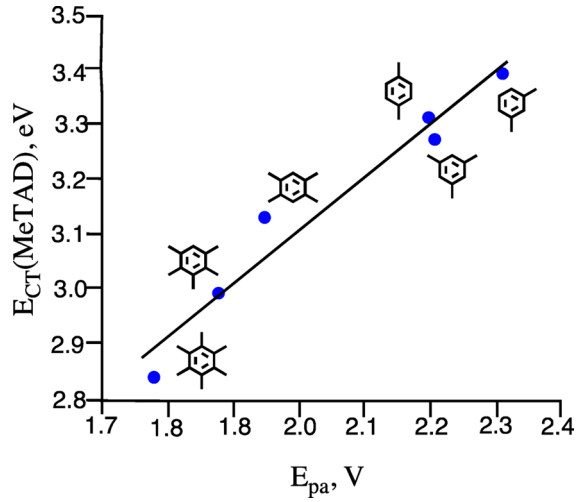

Figure 6. Correlation of the measured peak potentials (E_{pa}) of the various methylated benzene substrates with the observed energies of the charge-transfer absorption bands formed with **2** (E_{CT}(MeTAD)).

As with the correlation with ionization potential energies (Figure 3), the correlation of decreasing E_{CT}(MeTAD) with decreasing E_{pa} is further evidence for the charge-transfer nature of the observed UV−vis absorption bands.

The differences in potential between each of the aromatic substrates and **2** were used in eq 1 to calculate the $\Delta G'$ values for conversion of each of the CT complexes to the RA of **2** and RC of the aromatic substrate. These values are collected in

dx.doi.org/10.1021/jo4001417 | J. Org. Chem. 2013, 78, 4697−4707

Table 3. All of the electron-rich methoxy-substituted aromatic substrates afforded relatively large negative $\Delta G'$ values, ranging from −0.83 eV (−19.1 kcal/mol) for 1,4-dimethoxybenzene to −0.48 eV (−11.1 kcal/mol) for *m*-methylanisole. The methylated substrates exhibited large $\Delta G'$ values for highly methylated substrates (e.g., hexamethylbenzene at −0.57 eV (−13.1 kcal/mol)) but a value near 0 eV for the simple dimethylated arene *m*-xylene. However, for all of the arenes investigated, photoexcitation of the CT complex leading to electron transfer appears to be feasible.

6. Role of Radical Cation Intermediates in Determining the Product Distribution. During his investigation of the dichotomy between routes of formation of ring- and benzylic-substituted products in the reaction of aromatics with thallium(III) electrophiles,[13] Kochi described the correlation between the formation of the two types of thallated products (ring versus benzylic substituted) with the spin densities (inferred from the SOMO) on the aromatic carbons of the transient RCs.[13d] In particular, it was noted that when considerable spin density was predicted for unsubstituted carbons of the RCs of the aromatic substrates, ring substitution was facilitated. More recently, MacLachlan demonstrated that the spin density map of the aromatic RC intermediate formed via electron transfer from 1,2-dimethoxybenzene to the NO_2^+ electrophile could be used to explain the unusual regioselectivity of the aromatic substitution process.[30]

Taking Kochi's concept one step further, we calculated whole-molecule spin density maps of the RCs that would be generated upon photoinduced electron transfer to **2** from the various aromatic substrates explored in this study (Figure 7). We employed DFT methods at the UB3LYP/6-31G* level. Calculations at this level of theory have been demonstrated to satisfactorily replicate experimentally determined data, including spin densities, for aromatic radicals and RCs.[31] We discovered an exceptionally strong correlation between the predicted spin densities and the resulting product distributions from the reactions. For example, the spin density maps for the RCs of 1,3,5-trimethoxybenzene (**20**), 1,3-dimethoxybenzene (**21**), and 3,5-dimethoxytoluene (**22**) showed concentrated spin densities at an unsubstituted position of the aromatic ring. In all three cases a high yield of a 1-arylurazole was obtained as the sole product. In addition, for 3,5-dimethoxytoluene a single regioisomer (**12**) was obtained, which correlates to substitution at the aromatic carbon with the highest predicted spin density (i.e., adjacent to the methyl group). We did not observe formation of the other possible regioisomer (i.e., opposite the methyl group), for which the spin density map predicts no significant spin.

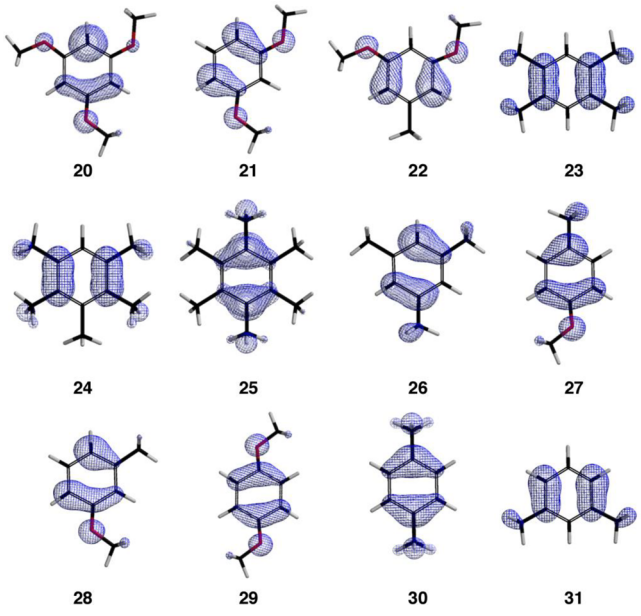

Figure 7. Spin density maps of the radical cations of aromatic substrates calculated at the UB3LYP/6-31G* level. The spin density maps for radical cations correlate as follows: **20**, trimethoxybenzene; **21**, 1,3-dimethoxybenzene; **22**, 3,5-dimethoxytoluene; **23**, durene; **24**, pentamethylbenzene; **25**, hexamethylbenzene; **26**, mesitylene; **27**, 4-methylanisole; **28**, 3-methylanisole; **29**, 1,4-dimethoxybenzene; **30**, *p*-xylene; **31**, *m*-xylene.

In contrast, the spin density maps of the RCs of durene (**23**), pentamethylbenzene (**24**), and hexamethylbenzene (**25**) predicted no spin density at unsubstituted positions on the aromatic ring and no 1-arylurazole products were observed. There was, however, predicted spin density at the benzylic hydrogens of the methyl groups of each of these RCs. Hydrogen abstraction by the RA of **2** could lead to the observed benzylic urazole products (vide infra). Notice that there is no predicted spin density on the benzylic hydrogens of the RC of **22** and no benzylic substitution was observed. The failure to produce a 1-arylurazole product from pentamethylbenzene is particularly striking. Pentamethylbenzene is the most reactive of the methylated benzenes toward electrophilic aromatic substitution, being about 5 times more reactive toward chlorination than the second most reactive arene, mesitylene.[32] The spin density maps, however, clearly predict the respective regiochemical outcomes from the photochemical reactions of the two substrates with **2**. In contrast to the case for **24**, the spin density map of the mesitylene RC (**26**) places considerable spin density at the unsubstituted carbons of the aromatic ring and lesser density at the benzylic methyl hydrogen atoms. Thus, unlike the reaction with pentamethylbenzene, products of both ring and side-chain substitution were observed. Furthermore, the higher percentage of ring substitution (70% of product) relative to benzylic substitution (30%) is consistent with the relative amounts of spin densities. For the 4-methylanisole RC (**27**), there is a predicted concentration of spin density at the aromatic carbon bearing the methyl group (for which no substitution is possible), a more diffuse spin density on the positions ortho to the methoxy group, and negligible spin density ortho to the methyl group. However, considerable spin density is observed at the benzylic hydrogens. In this case formation of the benzylic urazole product **17a** (83% of product) far outweighed formation of the ring-substituted product **17b** (17%). Furthermore, the regiochemistry of the ring-substituted product, i.e. substitution ortho to the methoxy groups to form **17b**, is that expected on the basis of the spin density. It is interesting to compare this finding to the reaction of 3-methylanisole. Both compounds have very similar peak potentials (1.83 V for *p*-methylanisole and 1.89 V for *m*-methylanisole); however, the spin density maps for the intermediate RCs predict very different experimental results. Unlike **27**, very little spin density is predicted at the benzylic hydrogens of the RC **28**, whereas considerable density is observed at the position ortho to the methyl group, and a more diffuse cloud at either position ortho to the methoxy group. Experimentally, only products of ring substitution were observed, as predicted by the spin density map. Furthermore,

dx.doi.org/10.1021/jo4001417 | J. Org. Chem. 2013, 78, 4697−4707

reaction took place primarily at the position ortho to the methyl group to afford **11a** (78% of product), as would be expected, with a lesser amount (22%) of a mixture of the two other ring-substituted 1-arylurazoles, **11b,c**, resulting from substitution ortho to the methoxy group.

We are unable to readily explain the lack of reactivity of 1,4-dimethoxybenzene under the reaction conditions, since its RC (**29**) places spin density at all four positions ortho to the two methoxy groups, suggesting a gravitation toward formation of a 1-arylurazole. The spin density cloud for **29** is especially diffuse, however. Perhaps this diffusiveness renders it unattractive to the triazolinedione radical anion and, as a result, collapse to form the Wheland intermediate is slow relative to back electron transfer. Additionally, as discussed earlier, 1,4-dimethoxybenzene was the one aromatic substrate studied by cyclic voltammetry for which a quasi-reversible redox couple was observed, which further indicates the reluctance of the 1,4-dimethoxybenzene RC to engage in reactions with nucleophiles. Interestingly, similar to that of **29**, the spin density map for the RC of *p*-xylene (**30**) also places diffuse spin density at the four aromatic carbon atoms ortho to the methyl groups. Again, very little reactivity was observed at the positions ortho to the methyls and the 1-arylurazole product **18b** was only a minor product (6% of product). However, the spin density map *does* indicate considerable spin density at the methyl hydrogens, and formation of the benzylic-substituted product **18a** predominates (94% of product). These results indicate that both the location and concentration of the spin density are important factors to consider when using spin density maps to predict product distributions.

The arene *m*-xylene is the one substrate for which the spin density prediction of the incipient RC (**31**) was not a wholly satisfactory predictor of product distribution. The spin density map reveals considerable spin density at the C4 and C6 positions as well as on the methyl groups. The major 1-arylurazole product **19a** clearly derives from reaction of the RA of **2** at the C4/C6 positions. Also isolated, as expected, was the benzylic urazole product **19c**. Whereas compounds **19a,c** were both expected on the basis of the spin density map, not predicted was formation of 1-arylurazole **19b**. Indeed, the spin density map shows absolutely no density at C2 of the RC ring. Recall, however, that *m*-xylene was the aromatic substrate with the least negative predicted $\Delta G'$ value of −0.05 eV (−1.2 kcal/mol) (Table 3). It is possible that an alternative mechanism of formation, such as direct electrophilic attack of photoactivated **2** on the aromatic ring, competes with the electron-transfer process and is responsible for the formation of **19b**.

7. Hydrogen Atom Transfer versus Proton Transfer from within the Charge-Transfer Complex. The strong correlation of product distribution with the spin density maps suggests the possibility that rather than a proton transfer from the RC to the RA of **2** as shown in route ii of Scheme 4, perhaps a hydrogen atom transfer is favored as shown in route iii of Scheme 5. Such hydrogen-abstraction behavior would be similar to that observed in the photochemical reactions of **2** with ethers, as mentioned previously.[4c,5] The spin density map of the RA of **2** displays concentrated spin density on the 1,2-nitrogen atoms and to a lesser extent on the carbonyl oxygen atoms (Figure 8). Thus, it is reasonable to expect hydrogen atom abstraction by the RA from the benzylic methyl sites of the RCs for which sufficient spin density resides. The resulting benzylic carbocation is stabilized by strong resonance interactions, and the urazolyl anion is known to be easily

Scheme 5. Formation of 1-Arylurazoles via Hydrogen Atom Abstraction by the Radical Anion of 2

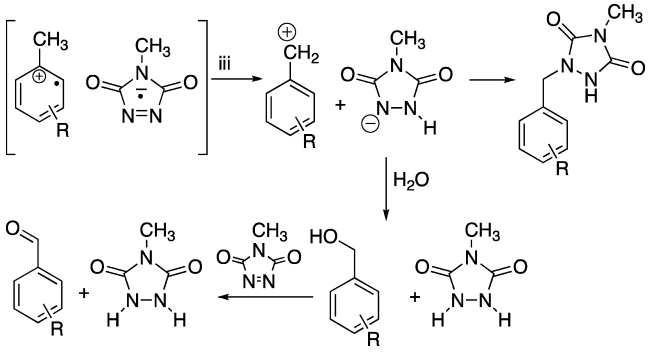

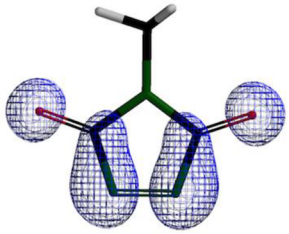

Figure 8. Spin density map for the radical anion of **2** calculated at the UB3LYP/6-31G* level.

formed (pK_a of *N*-methylurazole ~12).[20] In support of this mechanism, small amounts of substituted benzaldehydes were observed by ^{1}H NMR spectroscopy in the crude reaction mixtures of several of the reactions from which 1-arylurazole products were formed. Trapping of a benzylic carbocation intermediate formed in route iii by adventitious water to form the corresponding benzyl alcohol, followed by oxidation of the alcohol to the benzaldehyde by **2**, readily accounts for this finding (Scheme 5). Protonation of the urazolyl anion during trapping of the carbocation by water would lead to formation of *N*-methylurazole. Also, it is known that oxidation of benzyl alcohol to benzaldehyde by RTADs results in reduction of the RTAD to form the corresponding urazole.[33] Thus, this pathway could help account for the observation of *N*-methylurazole in the reactions in which benzylic substitution occurs.

■ CONCLUSION

In summary, visible light irradiation of MeTAD is capable of inducing reactivity with substituted benzenes in cases where no reaction takes place thermally. The observed products (1-arylurazoles and/or benzylic urazoles) are consistent with formation of a common intermediate, a radical ion pair formed from photoexcitation of an initially formed charge-transfer complex. The calculated spin density maps of the aromatic radical cation intermediates are excellent predictors of the product distributions observed.

■ EXPERIMENTAL SECTION

General Methods. Photochemical reactions were carried out in an in-house-designed apparatus consisting of an inner Pyrex cylindrical reaction vessel (2 cm × 150 cm) encased within an outer Pyrex vessel (4 cm × 190 cm), between which cool water was continually circulated. Visible light was provided by three 300 W incandescent bulbs strategically placed around the photochemical apparatus to maximize exposure of the reaction mixture to light. Column chromatography was conducted on silica gel (234−400 mesh) using

dx.doi.org/10.1021/jo4001417 | J. Org. Chem. 2013, 78, 4697−4707

compound-appropriate mixtures of hexanes and EtOAc as eluent. Thin-layer chromatography was performed on precoated silica gel plates and visualized by ultraviolet light and/or I_2 vapor. ^{1}H and ^{13}C NMR spectra were obtained on a 400 MHz NMR spectrometer. Chemical shifts are reported in units of parts per million downfield from TMS. Elemental analyses were performed by a commercial laboratory. High-resolution mass spectral analysis was performed via GC-MS (TOF EI). *N*-Methyl-1,3,5-triazolinedione (**2**) was synthesized via oxidation of commercially obtained *N*-methylurazole with N_2O_4 according to the literature and sublimed before use.[34,35] All other chemicals and solvents were obtained from commercial sources and used without further purification.

General Procedure: Photochemical Reactions of *N*-Methyl-1,2,4-triazoline-3,5-dione (2) with Substituted Benzenes. A solution of a substituted benzene (1.5 mmol) in 5 mL of CH_2Cl_2 was transferred to the reaction vessel of the photochemical apparatus described in General Methods. To this was added a solution of **2** (113 mg, 1 mmol) in 5 mL of CH_2Cl_2. The reaction vessel was sealed with a stopper and cool water circulated within the apparatus. Irradiation with three 300 W incandescent bulbs, arranged within 1 cm of the outside wall of the apparatus, was initiated and continued until the pinkish red color of the reaction mixture was just bleached. The reaction mixture was transferred to a 25 mL RBF, the solvent removed in vacuo, and the reaction mixture subjected to column chromatography.

*1-(2,4,6-Trimethoxybenzene)-4-methyl-1,2,4-triazoline-3,5-dione (**9**).*[3] Upon completion of reaction with 1,3,5-trimethoxybenzene (0.252 g) after 0.5 h, the solvent was removed and the residue recrystallized directly from EtOH to afford 0.244 g (87% yield) of **9** as colorless crystals, mp 252−253 °C: IR (cm^{-1}) 3152 (N−H), 3041, 2986, 1767, 1688, 1131; ^{1}H NMR (DMSO-d_6) δ 2.94 (s, 3H), 3.75 (s, 6H), 3.82 (s, 3H), 6.30 (s, 2H), 10.68 (br s, 1H); ^{13}C NMR (DMSO-d_6) δ 162.1, 158.7, 153.5, 152.7, 105.4, 91.1, 56.1, 55.7, 24.7.

*1-(2,4-Dimethoxybenzene)-4-methyl-1,2,4-triazoline-3,5-dione (**10**).*[3] Upon completion of reaction with 1,3-dimethoxybenzene (0.202 g) after 3 h, column chromatography afforded 0.198 g (79% yield) of **10** as a white solid, mp 185−186 °C: ^{1}H NMR ($CDCl_3$) δ 3.15 (s, 3H), 3.82 (s, 3H), 3.85 (s, 3H), 6.49 (dd, J = 2.5, 8.5 Hz, 1H), 6.52 (d, J = 2.5 Hz, 1H), 7.41 (d, J = 8.5 Hz, 1H), 8.15 (br s, 1H); ^{13}C NMR ($CDCl_3$) δ 161.1, 155.4, 154.9, 152.5, 127.9, 117.4, 104.6, 99.7, 55.9, 55.7, 25.3.

*1-(4-Methoxy-2-methylbenzene)-4-methyl-1,2,4-triazoline-3,5-dione (**11a**).*[3] Upon completion of reaction with 3-methylanisole (0.183 g) after 18 h, column chromatography afforded 0.186 g (79% yield) of a mixture of regioisomeric 1-arylurazoles **11a−c** as a foamy white solid. The major product, **11a**, exhibited spectral data identical with those of the product previously isolated from the acid-catalyzed reaction of **2** with 3-methoxytoluene: ^{1}H NMR (DMSO-d_6) δ 2.20 (s, 3H), 2.96 (s, 3H), 3.77 (s, 3H), 6.84 (dd, J = 3.1, 8.5 Hz, 1H), 6.90 (d, J = 3.1 Hz, 1H), 7.26 (d, J = 8.5 Hz, 1H), 10.87 (br s, 1H); ^{13}C NMR ($CDCl_3$) δ 160.0, 154.8, 152.2, 138.0, 128.1, 127.0, 116.2, 112.2, 55.5, 25.3, 18.0.

In addition to **11a** (~86% of the product mixture according to integration in the ^{1}H NMR spectrum), the crude reaction mixture suggested two other regioisomeric products in a ratio of ~1:1 tentatively assigned structures **11b,c** (see text). The ^{1}H NMR spectrum of the crude mixture is provided in the Supporting Information.

*1-(2,4-Dimethoxy-6-methylbenzene)-4-methyl-1,2,4-triazoline-3,5-dione (**12**).*[3] Upon completion of reaction with 3,5-dimethoxytoluene (0.228 g) after 1 h, column chromatography afforded 0.257 g (97% yield) of **12** as a white solid, mp 165−166 °C: ^{1}H NMR ($CDCl_3$) δ 2.25 (s, 3H), 3.10 (s, 3H), 3.74 (s, 3H), 3.79 (s, 3H), 6.31 (d, J = 2.5 Hz, 1H), 6.35 (d, J = 2.5 Hz, 1H), 9.10 (br s, 1H); ^{13}C NMR ($CDCl_3$) δ 161.5, 157.6, 155.4, 153.1, 140.8, 115.6, 106.4, 97.1, 55.9, 55.5, 25.3, 18.0.

*1-(2,4,6-Trimethylbenzene)-4-methyl-1,2,4-triazoline-3,5-dione (**13a**).*[3] Upon completion of reaction with mesitylene (0.180 g) after 10 h, column chromatography afforded 0.182 g (78% yield) of **13a,b** as an inseparable mixture in a ratio (by ^{1}H NMR integration) of 2.3:1, respectively. The major product, **13a**, exhibited spectral data identical with those of the product previously isolated from the acid-catalyzed reaction of **2** with mesitylene as a white solid, mp 134−136 °C: ^{1}H NMR ($CDCl_3$) δ 2.13 (s, 6H), 2.28 (s, 3H), 3.06 (s, 3H), 6.89 (s, 2H), 9.49 (br s, 1H); ^{13}C NMR ($CDCl_3$) δ 154.8, 151.3, 140.2, 137.9, 129.5, 129.3, 25.3, 21.1, 17.6.

The ^{1}H and ^{13}C NMR signals in the crude spectra corresponding to **13b** matched those of an independently synthesized compound (see below).

*1-(2,4,5-Trimethylbenzyl)-4-methyl-1,2,4-triazoline-3,5-dione (**14**).* Upon completion of reaction with 1,2,4,5-tetramethylbenzene (0.201 g) after 8 h, column chromatography afforded 0.141 g (57% yield) of **14** as a white solid, mp 175−176 °C: IR (cm^{-1}) 3198 (N−H), 2992, 1779, 1676; ^{1}H NMR ($CDCl_3$) δ 2.19 (s, 6H), 2.27 (s, 3H), 3.02 (s, 3H), 4.59 (s, 2H), 6.94 (s, 1H), 6.99 (s, 1H), 8.00 (br s, 1H); ^{13}C NMR ($CDCl_3$) δ 155.0, 154.0, 137.1, 134.4, 134.3, 132.2, 131.1, 129.1, 48.4, 25.2, 19.3, 19.2, 18.4. Anal. Calcd for $C_{13}H_{17}N_3O_2$: C, 63.12; H, 6.93; N, 17.00. Found: C, 62.86; H, 7.08; N, 16.73.

*Benzylic Substituted Products from Reaction with Pentamethylbenzene (**15a−c**).* Upon completion of reaction with pentamethylbenzene (0.224 g) after 5 h, column chromatography afforded 0.1064 g (41% yield) of an inseparable mixture of urazoles **15a−c** as a white solid. Using the signal integrations from the ^{1}H NMR spectrum of the crude mixture (provided in the Supporting Information), the spectra for each of the individual isomers could be determined. Minor isomer **15c**: ^{1}H NMR ($CDCl_3$) δ 2.21 (s, 6H), 2.24 (s, 6H), 2.99 (s, 3H), 4.75 (s, 2H), 6.93 (s, 1H), 8.05 (br s, 1H). The other two regioisomers, **15a,b** could not be clearly differentiated. However, one was present in greater amount than the other. Major isomer: ^{1}H NMR ($CDCl_3$) δ 2.14 (s, 3H), 2.22 (s, 3H), 2.27 (s, 3H), 2.31 (s, 3H), 2.99 (s, 3H), 4.70 (s, 2H), 6.83 (s, 1H), 8.05 (br s, 1H). Remaining isomer: ^{1}H NMR ($CDCl_3$) δ 2.17 (s, 3H), 2.19 (s, 3H), 2.23 (s, 3H), 2.24 (s, 3H), 2.97 (s, 3H), 4.61 (s, 2H), 8.05 (br s, 1H). Elemental analysis was conducted on the mixture of isomers. Anal. Calcd for $C_{14}H_{19}N_3O_2$: C, 64.33; H, 7.33; N, 16.09. Found: C, 64.34; H, 7.45; N, 15.94.

*1-(2,3,4,5,6-Pentamethylbenzyl)-4-methyl-1,2,4-triazoline-3,5-dione (**16**).* Upon completion of reaction with hexamethylbenzene (0.243 g) after 8 h, column chromatography afforded 0.153 g (56% yield) of **16** as a white solid, mp 237−239 °C: ^{1}H NMR ($CDCl_3$) δ 2.24 (s, 6H), 2.26 (s, 3H), 2.32 (s, 6H), 3.10 (s, 3H), 4.83 (s, 2H), 6.40 (br s, 1H); ^{13}C NMR ($CDCl_3$) δ 155.0, 154.0, 136.0, 133.7, 133.3, 126.5, 45.7, 25.2, 17.1, 16.8, 16.5. Anal. Calcd for $C_{15}H_{21}N_3O_2$: C, 65.42; H, 7.69; N, 15.27. Found: C, 65.16; H, 7.83; N, 14.93.

*1-(4-Methoxybenzyl)-4-methyl-1,2,4-triazoline-3,5-dione (**17a**) and 1-(2-Methoxy-5-methylbenzyl)-4-methyl-1,2,4-triazoline-3,5-dione (**17b**).* Upon completion of reaction with 4-methylanisole (0.183 g) after 24 h, column chromatography afforded 0.101 g (43% yield) of a difficultly separable mixture of **17a,b** in an 83:17 ratio, respectively. When several such product mixtures were combined and subjected to further column chromatography, it was possible to isolate sufficient amounts of pure fractions of each compound for characterization by combining very early (**17b**) and very late (**17a**) fractions about the region where they nearly coelute. Compound **17a** was isolated as a white solid, mp 147−148 °C: ^{1}H NMR ($CDCl_3$) δ 3.03 (s, 3H), 3.79 (s, 3H), 4.59 (s, 2H), 6.86 (d, J = 8.5 Hz, 2H), 7.24 (d, J = 8.5 Hz, 2H), 8.1 (br s, 1H); ^{13}C NMR ($CDCl_3$) δ 159.8, 155.0, 154.4, 130.2, 126.0, 114.3, 55.3, 50.2, 25.2. Anal. Calcd for $C_{11}H_{13}N_3O_3$: C, 56.15; H, 5.57; N, 17.87. Found: C, 55.83; H, 5.48; N, 17.72. Compound **17b** was isolated as a white solid, mp 147−148 °C: ^{1}H NMR ($CDCl_3$) δ 2.31 (s, 3H), 3.17 (s, 3H), 3.88 (s, 3H), 6.88 (d, J = 8.4 Hz, 1H), 7.11 (dd, J = 1.8, 8.4 Hz, 1H), 7.45 (d, J = 1.8 Hz, 1H), 8.3 (br s, 1H); ^{13}C NMR ($CDCl_3$) δ 154.6, 151.6, 150.9, 131.0, 129.6, 125.9, 123.9, 111.9, 56.0, 25.3, 20.5. Anal. Calcd for $C_{11}H_{13}N_3O_3$: C, 56.15; H, 5.57; N, 17.87. Found: C, 55.73; H, 5.45; N, 17.51.

*1-(4-Methylbenzyl)-4-methyl-1,2,4-triazoline-3,5-dione (**18a**) and 1-(2,5-Dimethylbenzyl)-4-methyl-1,2,4-triazoline-3,5-dione (**18b**).* Upon completion of reaction with *p*-xylene (0.160 g) after 14 h, column chromatography afforded 0.065 g (30% yield) of **18a** as a white solid, mp 149−150 °C: ^{1}H NMR ($CDCl_3$) δ 2.33 (s, 3H), 3.02 (s, 3H), 4.61 (s, 2H), 7.14 (d, J = 8.0 Hz, 2H), 7.19 (d, J = 8.0 Hz,

dx.doi.org/10.1021/jo4001417 | J. Org. Chem. 2013, 78, 4697−4707

2H), 8.27 (br s, 1H); ^{13}C NMR ($CDCl_3$) δ 154.9, 154.2, 138.3, 131.1, 129.6, 128.6, 50.3, 25.2, 21.1; HRMS (TOF EI) m/z $[M]^+$ calcd for $C_{11}H_{13}N_3O_2$ 219.1008, found 219.1017. Also isolated was 5 mg (2% yield) of **18b** as a white solid: IR (cm^{-1}) 3154 (N−H), 2950, 1776, 1694; ^{1}H NMR ($CDCl_3$) δ 2.30 (s, 3H), 2.32 (s, 3H), 3.15 (s, 3H), 7.09 (dd, J = 1.2, 7.8 Hz, 1H), 7.15 (d, J = 1.2 Hz, 1H), 7.17 (d, J = 7.8 Hz, 1H) (the N−H signal was particularly broad for this sample; the presence of the N−H was confirmed by the IR spectrum above); ^{13}C NMR ($CDCl_3$) δ 155.1, 152.4, 136.9, 134.6, 132.7, 131.3, 129.9, 126.1, 25.5, 20.8, 17.5; HRMS (TOF EI) m/z $[M]^+$ calcd for $C_{11}H_{13}N_3O_2$ 219.1008, found 219.1003.

*1-(2,4-Dimethylbenzyl)-4-methyl-1,2,4-triazoline-3,5-dione (**19a**),*[3] *1-(2,6-Dimethylbenzyl)-4-methyl-1,2,4-triazoline-3,5-dione (**19b**), and 1-(3-Methylbenzyl)-4-methyl-1,2,4-triazoline-3,5-dione (**19c**).* Upon completion of reaction with *m*-xylene (0.159 g) after 11 h, column chromatography afforded 0.131 g (62% yield) of a nearly inseparable mixture of urazoles **19a−c** as a white solid. Compound **19a** was readily identified by comparison of its NMR spectra with those of the known compound: ^{1}H NMR ($CDCl_3$) δ 2.30 (s, 3H), 2.33 (s, 3H), 3.13 (s, 3H), 7.05 (d, J = 7.9 Hz, 1H), 7.10 (s, 1H), 7.19 (d, J = 7.9 Hz, 1H), 8.15 (br s, 1H). ^{13}C NMR ($CDCl_3$) δ 155.1, 152.3, 139.3. 135.7, 132.1, 127.6, 125.8, 25.4, 21.1, 17.9. Chromatographic fractions could be enriched in mixtures of **19a,b** for analysis by NMR spectroscopy. The structure for **19b** was assigned by subtracting the signals due to **19a** from the ^{1}H and ^{13}C NMR spectra: ^{1}H NMR ($CDCl_3$) δ 2.19 (s, 6H), 3.07 (s, 3H), 7.09 (d, J = 7.8 Hz, 2H), 7.22 (t, J = 7.8 Hz, 1H), 9.4 (br s, 1H); ^{13}C NMR ($CDCl_3$) δ 154.8, 151.3, 138.3, 131.9, 130.2, 128.8, 25.3, 17.8. The NMR spectra for **19c** were identical with those of the independently prepared compound (see below).

General Procedure: Thermal Reactions of *N*-Methyl-1,3,5-triazolinedione (2) with Substituted Benzenes. A solution of a substituted benzene (1.5 mmol) in 5 mL of CH_2Cl_2 was transferred to a clean, dry 25 mL RBF. To this solution, with stirring, was added a solution of **2** (113 mg, 1 mmol) in 5 mL of CH_2Cl_2. The reaction mixture was protected from light by wrapping in aluminum foil and allowed to run for the designated time. Upon completion of the reaction the solvent was removed in vacuo, and the reaction mixture subjected to column chromatography.

Thermal Reaction with 1,3,5-Trimethoxybenzene. According to the general procedure, 1,3,5-trimethoxybenzene (0.252 g) was allowed to react with **2** until the red color of **2** was bleached (9 h). The solvent was removed and the residue recrystallized directly from EtOH to afford 0.257 g (91% yield) of **9** as colorless crystals.

Thermal Reaction with 1,3-Dimethoxybenzene. According to the general procedure, 1,3-dimethoxybenzene (0.202 g) was allowed to react with **2** for 4 days. The solvent was removed and the residue subjected to column chromatography, from which 0.116 g (46% yield) of **10** was isolated as a white solid.

*1-(3,5-Dimethylbenzyl)-4-methyl-1,2,4-triazoline-3,5-dione (**13b**).* Following the procedure of Wilson,[34] triethylamine (194 μL, 1.4 mmol) was added to 0.64 g (5.6 mmol) of *N*-methylurazole in 25 mL of dry THF. The resulting mixture was heated to 40 °C for 1 h. Solid 3,5-dimethylbenzyl bromide (0.28 g, 1.4 mmol) was added to the mixture, and heating was continued for 20 h. The reaction mixture was cooled to room temperature and poured into 50 mL of NH_4Cl/brine. The THF layer was separated and the aqueous layer washed with 3 × 20 mL of EtOAc. The combined organic fractions were dried over Na_2SO_4, filtered, and concentrated. Column chromatography (EtOAc) afforded 90.4 mg (28% yield) of **13b** as a white solid, mp 147−148 °C: ^{1}H NMR (DMSO-d_6) δ 2.25 (s, 6H), 2.89 (s, 3H), 4.51 (s, 2H), 6.86 (s, 2H), 6.93 (s, 1H), 10.5 (br s, 1H). ^{13}C NMR ($CDCl_3$) δ 154.9, 154.1, 138.6, 133.9, 130.1, 126.4, 50.4, 25.2, 21.2. Anal. Calcd for $C_{12}H_{15}N_3O_2$: C, 61.77; H, 6.48; N, 18.02. Found: C, 61.64; H, 6.47; N, 17.65.

*1-(3-Methylbenzyl)-4-methyl-1,2,4-triazoline-3,5-dione (**19c**).* As above, triethylamine (194 μL, 1.4 mmol) was added to 0.64 g (5.6 mmol) of *N*-methylurazole in 25 mL of dry THF. The resulting mixture was heated to 40 °C for 1 h. 3-Methylbenzyl bromide (0.26 g, 1.4 mmol) was added via syringe to the mixture, and heating was continued for 20 h. The reaction mixture was cooled to room temperature and poured into 50 mL of NH_4Cl/brine. The THF layer was separated and the aqueous layer washed with 3 × 20 mL of EtOAc. The combined organic fractions were dried over Na_2SO_4, filtered, and concentrated. Column chromatography (EtOAc) afforded 61 mg (20% yield) of **19c** as a white solid, mp 113−114 °C: ^{1}H NMR ($CDCl_3$) δ 2.33 (s, 3H), 3.01 (s, 3H), 4.61 (s, 2H), 7.06−7.14 (m, 3H), 7.21 (t, J = 7.6 Hz, 1H), 8.50 (v br s, 1H); ^{13}C NMR ($CDCl_3$) δ 155.0, 154.1, 138.7, 134.0, 129.3, 129.2, 128.8, 125.6, 50.5, 25.2, 21.3; HRMS (TOF EI) m/z $[M]^+$ calcd for $C_{11}H_{13}N_3O_2$ 219.1008, found 219.1011.

UV−Vis Spectroscopic Analysis of Charge-Transfer Complexes. A 30 mM stock solution of *N*-methyl-1,2,4-triazoline-3,5-dione (**2**) was prepared by dissolving 85 mg (0.75 mmol) of freshly sublimed **2** in 25 mL of dry CH_2Cl_2. To 1 mL of this solution in a cuvette was added a solution of 3 mmol of the aromatic substrate in 2 mL of CH_2Cl_2. The contents were briefly mixed, and the UV−vis spectrum was collected. Absorbances due to the charge-transfer complexes were obtained by subtracting the UV−vis spectrum of **2** (10 mM) from the spectra of the mixtures.

Electrochemical Measurements. High-purity acetonitrile was dried over activated 3 Å sieves under dry nitrogen for 24−48 h before use. Tetrabutylammonium hexafluorophosphate was dried in vacuo for 24 h and then dissolved in dried acetonitrile to make a 0.1 M supporting electrolyte solution. An oven-dried 15 mL vial was used to contain 10 mL of electrolyte, with a customized Teflon cap holding the three electrodes used. A commercial reference electrode was used, consisting of a glass body containing a silver wire immersed in saturated aqueous AgCl in 4 M KCl. The porous glass tip of the reference electrode was rinsed with dry acetonitrile prior to insertion into the cell. A 3 mm glassy-carbon-disk electrode was polished with an aqueous slurry of 0.05 μm alumina, followed by sonication and rinsing with deionized water. This working electrode and a platinum-wire counter electrode were also rinsed with dry acetonitrile before insertion into the cell. The electrolyte in the assembled cell was purged with ultrahigh-purity nitrogen, and the nitrogen atmosphere was maintained for all experiments.

Cyclic voltammetry was performed at 0.1 V/s. After the stability of the solvent was verified to the upper potential limit, substances to be analyzed were introduced to give final concentrations of 1−3 mM. Ferrocene was added at 0.5 mM as an internal standard following all measurements. The average ferrocene potential under these conditions was measured at 0.470 V versus the reference electrode used. Where corrections of potentials to the standard hydrogen electrode (SHE) have been made, a potential of 0.624 V vs SHE was assumed for the potential of ferrocene.[24] Measurements were made at 22 °C. Voltammetry was collected following the convention in which anodic processes (i.e., oxidation of substrate) are assigned a positive current.

Computations. All computations were performed using Spartan '04. DFT calculations were conducted at the UB3LYP/6-31G* level. Generally, the structures of the neutral aromatic substrates were first minimized and served as a starting point for the optimization of the radical cation structure. Frequency calculations were carried out at the same level of theory to ensure that the geometry represented a true minimum (i.e., no imaginary frequencies). Spin expectation values $\langle S^2 \rangle$ (see the Supporting Information) suggested no appreciable spin contamination for any of the radical cations.

■ ASSOCIATED CONTENT

Supporting Information

Figures and tables giving ^{1}H and ^{13}C NMR spectra for all fully characterized urazole products and some mixtures and additional details on computations, including coordinates for computed structures. This material is available free of charge via the Internet at http://pubs.acs.org.

dx.doi.org/10.1021/jo4001417 | J. Org. Chem. 2013, 78, 4697−4707

AUTHOR INFORMATION

Corresponding Author

*E-mail for G.W.B.: gbreton@berry.edu.

Notes

The authors declare no competing financial interest.

ACKNOWLEDGMENTS

This material is based upon work supported by the National Science Foundation under CHE-1125616. G.W.B. thanks the Chemistry and Biochemistry Department at the University of Arizona for providing HRMS analysis through their Research Support and Outreach Program and also the Berry College Faculty Development Grant program for support of this research.

REFERENCES

(1) (a) Ruschig, H.; Schmitt, K.; Ther, L.; Pfaff, W. GB Patent 973359, 1962; *Chem. Abstr.* **1962**, 456301. (b) Mitchell, C. L.; Keasling, H. H.; Gross, E. G. *J. Am. Pharm. Assoc.* **1959**, *48*, 122−126. (c) Schmitt, K. DE Patent 1135478, 1962; *Chem. Abstr.* **1963**, 8912.

(2) Pirkle, W. H.; Gravel, P. L. *J. Org. Chem.* **1978**, *43*, 808−815.

(3) Breton, G. W. *Tetrahedron Lett.* **2011**, *52*, 733−735.

(4) (a) Risi, F.; Pizzala, L.; Carles, M.; Verlaque, P.; Aycard, J. P. *J. Org. Chem.* **1996**, *61*, 666−670. (b) Pirkle, W. H.; Stickler, J. C. *J. Am. Chem. Soc.* **1970**, *92*, 7497−7499. (c) Wamhoff, H.; Wald, K. *Chem. Ber.* **1977**, *110*, 1699−1715.

(5) Risi, F.; Alstanei, A. M.; Volanschi, E.; Carles, M.; Pizzala, L.; Aycard, J. P. *Eur. J. Org. Chem.* **2000**, 617−626.

(6) (a) Kjell, D. P.; Sheridan, R. S. *J. Am. Chem. Soc.* **1984**, *106*, 5368−5370. (b) Kjell, D. P.; Sheridan, R. S. *J. Photochem.* **1985**, *28*, 205−213. (c) Hamrock, S. J.; Sheridan, R. S. *Tetrahedron Lett.* **1988**, *29*, 5509−5512. (d) Hamrock, S. J.; Sheridan, R. S. *J. Am. Chem. Soc.* **1989**, *111*, 9247−9249.

(7) Breton, G. W.; Newton, K. A. *J. Org. Chem.* **2000**, *65*, 2863−2869.

(8) Angermund, K.; Bunte, R.; Goddard, R.; Leitich, J.; Polansky, O. E.; Zander, M. *Chem. Ber.* **1988**, *121*, 1647−1650.

(9) Ulmer, L.; Siedschlag, C.; Mattay, J. *Eur. J. Org. Chem.* **2003**, 3811−3817.

(10) See, for example: (a) Squillacote, M. E.; Garner, C.; Oliver, L.; Mooney, M.; Lai, Y.-L. *Org. Lett.* **2007**, *9*, 5405−5408. (b) Burger, U.; Mentha, Y. G.; Millasson, P.; Lottaz, P. A.; Mareda, J. *Helv. Chim. Acta* **1989**, *72*, 1722−1728. (c) Amey, R. L.; Smart, B. E. *J. Org. Chem.* **1981**, *46*, 4090−4092.

(11) (a) Kuhrau, M.; Stadler, R. *Makromol. Chem.* **1990**, *191*, 1787−1798. (b) Hall, J. H.; Kaler, L.; Herring, R. *J. Org. Chem.* **1984**, *49*, 2579−2582. (c) Hall, J. H. *J. Org. Chem.* **1983**, *48*, 1708−1712. (d) Zander, M. *Chem.-Ztg.* **1975**, *99*, 92−93.

(12) All NMR data predictions were performed using ACD/Laboratories NMR Predictor Suite v.12.

(13) (a) Rosokha, S. V.; Kochi, J. K. *J. Am. Chem. Soc.* **2001**, *123*, 8985−8999. (b) Bosch, E.; Kochi, J. K. *J. Org. Chem.* **1994**, *59*, 3314−3325. (c) Kim, E. K.; Bockman, T. M.; Kochi, J. K. *J. Am. Chem. Soc.* **1993**, *115*, 3091−3104. (d) Lau, W.; Kochi, J. K. *J. Am. Chem. Soc.* **1986**, *108*, 6720−6732. (e) Lau, W.; Kochi, J. K. *J. Am. Chem. Soc.* **1984**, *106*, 7100−7112. (f) Kochi, J. K. *Tetrahedron Lett.* **1974**, *15*, 4305−4308. (g) Kim, E. K.; Bockman, T. M.; Kochi, J. K. *J. Am. Chem. Soc.* **1993**, *115*, 3091−3104. (h) Masnovi, J. M.; Sankararaman, S.; Kochi, J. K. *J. Am. Chem. Soc.* **1989**, *111*, 2263−2276.

(14) Lias, S. G. Ionization Energy Evaluation. In *NIST Chemistry WebBook*; Linstrom, P. J., Mallard, W. G., Eds.; National Institute of Standards and Technology, Gaithersburg, MD, NIST Standard Reference Database Number 69, http://webbook.nist.gov (retrieved March 29, 2013).

(15) Raner, K. D.; Lusztyk, J.; Ingold, K. U. *J. Phys. Chem.* **1989**, *93*, 564−570.

(16) See ref 11c for Hall's proposal for a thermal electron transfer between electron-rich aromatics and RTAD from within a charge-transfer complex.

(17) (a) Farid, S.; Dinnocenzo, J. P.; Merkel, P. B.; Young, R. H.; Shukla, D.; Guirado, G. *J. Am. Chem. Soc.* **2011**, *133*, 11580−11587. (b) Farid, S.; Dinnocenzo, J. P.; Merkel, P. B.; Young, R. H.; Shukla, D. *J. Am. Chem. Soc.* **2011**, *133*, 4791−4801.

(18) Pocius, A. V.; Yardley, J. T. *J. Am. Chem. Soc.* **1973**, *95*, 721−725.

(19) The value for the constant in eq 1 was estimated from Figure 5 in ref 17b.

(20) Bausch, M. J.; David, B. *J. Org. Chem.* **1992**, *57*, 1118−1124.

(21) Alstanei, A. M.; Hornoiu, C.; Aycard, J. P.; Carles, M.; Volanschi, E. *J. Electroanal. Chem.* **2003**, *542*, 13−21.

(22) See, for example: (a) Weinberg, N. L.; Weinberg, H. R. *Chem. Rev.* **1968**, *68*, 449−523. (b) Merkel, P. B.; Luo, P.; Dinnocenzo, J. P.; Farid, S. *J. Org. Chem.* **2009**, *74*, 5163−5173. (c) Howell, J. O.; Goncalves, J. M.; Amatore, C.; Klasinc, L.; Wightman, R. M.; Kochi, J. K. *J. Am. Chem. Soc.* **1984**, *106*, 3968−3976.

(23) Gritzner, G.; Kůta, J. *Pure Appl. Chem.* **1984**, *56*, 461−466.

(24) Pavlishchuk, V. V.; Addison, A. W. *Inorg. Chim. Acta* **2000**, *298*, 97−102.

(25) (a) Amatore, C.; Lefrou, C. *J. Electroanal. Chem.* **1992**, *325*, 239−246. (b) Zweig, A.; Hodgson, W. G.; Jura, W. H. *J. Am. Chem. Soc.* **1964**, *86*, 4124−4129.

(26) Bewick, A.; Edwards, G. J.; Mellor, J. M. *Justus Liebigs Ann. Chem.* **1978**, *1978*, 41−53.

(27) Schäfer, H. J. Electrolytic oxidative coupling. In *Organic Electrochemistry*; Lund, H., Hammerich, O., Eds.; Marcel Dekker: New York, 2001; pp 883−967.

(28) Le Berre, V.; Angely, L.; Simonet, J.; Mousset, G.; Bellec, M. *J. Electroanal. Chem.* **1987**, *218*, 173−185.

(29) Buck, R. P.; Wagoner, D. E. *J. Electroanal. Chem.* **1980**, *115*, 89−113.

(30) Shopsowitz, K.; Lelj, F.; MacLachlan, M. J. *J. Org. Chem.* **2011**, *76*, 1285−1294.

(31) (a) Qin, Y.; Wheeler, R. A. *J. Phys. Chem.* **1996**, *100*, 10554−10563. (b) Wu, Y. D.; Wong, C. L.; Chan, K. W. K.; Ji, G. Z.; Jiang, X. K. *J. Org. Chem.* **1996**, *61*, 746−750.

(32) (a) Koleva, G.; Galabov, B.; Wu, J. I.; Schaefer, H. F., III; Schleyer, P. v. R. *J. Am. Chem. Soc.* **2009**, *131*, 14722−14727. (b) Baciocchi, E.; Illuminati, G. *Gazz. Chim. Ital.* **1962**, *92*, 89−98.

(33) (a) Borhani, D. W.; Greene, F. D. *J. Org. Chem.* **1986**, *51*, 1563−1570. (b) Cookson, R. C.; Stevens, I. D. R.; Watts, C. T. *Chem. Commun.* **1966**, 744.

(34) Mallakpour, S. E. *J. Chem. Educ.* **1992**, *69*, 238−241.

(35) Wilson, R. M.; Hengge, A. *J. Org. Chem.* **1987**, *52*, 2699−2707.